THE ROWLAND INSTITUTE FOR SCIENCE
100 Cambridge Parkway
Cambridge, Massachusetts 02142 USA

Research Memo RIS No. 38r *December 9, 1986*

Strobe Imagery: A Scanning Model

by

Stewart W. Wilson

Abstract

An early suggestion of Grey Walter is combined with recent understanding of the retino-cortical mapping in a model to account for the principal imagery sometimes seen in uniform flashing lights. The model postulates dual linear cortical scan-like sampling processes whose interaction with the flash produces the images.

Existing explanations of the phenomena are reviewed, and a prediction which tests the model is presented.

Keywords and Phrases: vision, strobe imagery, cortex, retino-cortical mapping, scanning

1. Introduction

About thirty-five years ago Grey Walter (1950, 1953) suggested that the patterned imagery sometimes seen in uniform flashing lights could be accounted for by postulating a scanning process within the visual system. Such imagery had been noted as early as Purkinje (1823), whose observations were repeated by Helmholtz (1962). Walter (1953) summarizes as follows reports by subjects viewing a flashing strobe lamp with closed eyes: "The illusion is most marked when the flicker is between 8 and 25 flashes per second and takes a variety of forms. Usually it is a sort of pulsating check or mosaic, often in bright colors. At certain frequencies—around 10 per second—some subjects see whirling spirals, whirlpools, explosions, Catherine wheels."

Walter made an analogy with television to suggest how the imagery could result from a scanning process engaged in transferring "the spatial image which is received in the projection areas ... to the other areas for cognition." If a TV studio had perfectly featureless white walls, but they were illuminated by a flashing strobe, then if the strobe rate were near the frame rate of the TV system, definite patterns would nevertheless be seen on the receiver. In particular, the patterns would tend to reveal the path of the scanning beam. As for the brain, Walter suggested "the whirling spiral so many people see under flicker, is it not perhaps an indication of the very path taken by the scanning point ...?"

Walter's hypothesis is one of several on the origin of the stroboscopic patterns, none of which has been fully confirmed or disconfirmed. In making his suggestion, Walter could not benefit from later relevant information on the mapping relationship between the retina and primary visual cortex. Our objective is to extend Walter's basic idea in the light of this information, and to present a relatively simple quantitative mechanism which appears to account for much of the observed imagery.

2. Pattern Characteristics and Some Existing Explanations

Smythies (1957, 1959a&b, 1960) undertook a comprehensive investigation of "the natural history of the patterns", and discussed several previously proposed explanations. The 1957 paper classifies the imagery. "Common patterns were as follows: those based on straight lines, for example, checker-boards, grids, rasters, sets of parallel lines—horizontal and vertical—and herring-bone patterns; patterns based on curved lines or closed curves, for example, spirals, whirlpools, vortices, catherine wheels, sets of concentric circles, families of parabolas or sine waves and patterns like lines of magnetic force around a bar magnet; radial patterns, such as stars or snow flakes and ice-crystals; and lastly, maze, mosaic, or labyrinth patterns.

Almost all the patterns obtained could be classified into one of these groups. Notable features were their geometricity and their frequent movement, which was of many types—linear, oscillation, rotation, etc." The 1959b paper also mentions reports of a cross, flower or mandala figure.

Klüver (1942) sought a general structure common to all visual hallucinations. Drawing mainly from "the first stages of mescaline intoxication", he identified four classes of patterns, which he termed "form constants": "(a) grating, lattice, fretwork, filigree, honeycomb, or chessboard; (b) cobweb; (c) tunnel, funnel, alley, cone, or vessel; (d) spiral". In reviewing the literature, Klüver found some or all of the form constants to be present in a variety of other conditions, including drowsiness, entoptic phenomena, insulin hypoglycemia, illness, and rhythmic photostimulation of the eye. The list has since been extended (Siegel, 1977). Smythies (1960) discusses the strobe patterns in terms of Klüver's form constants and concludes they are "similar".

Explanations of the imagery fall into several categories.

> [1] Perhaps the oldest hypothesis is that one is seeing parts of the retinal anatomy, such as blood vessels, receptor cells, etc. (Edridge-Green, 1920). This could not hold for imagery which for example rotates, "explodes", or executes other large-scale movements. And the blood vessel pattern is not sufficiently regular geometrically. However, a central disk which is often observed could correspond to the macula. Also, as will be discussed later, the "cobweb" or mosaic whose elements grow with eccentricity may correspond to the decrease in cortical magnification factor with eccentricity.
>
> [2] Another line of thinking attributes the patterns to what might be termed "stimulus misinterpretation" (Smythies, 1960, on a personal communication from H. Barlow; Brown and Gebhard, 1948). The unusual abrupt on/off of the light is not recognized as such by the system, but is instead interpreted in terms of moving contours which are familiar and would have similar local effects on neurones (Barlow). Or the system may be "biased" toward spatial patterns over temporal changes (Brown and Gebhard). Smythies (1960) makes the point that the patterns may be "hypotheses" tried and discarded in turn in an attempt to identify a singular stimulus. One problem with this general view is that the frequently reported spiral pattern is not commonly encountered in daily visual life; therefore why should it be a common interpretation or hypothesis?

[3] A third view suggests that the patterns may represent spontaneous cortical activity triggered by or in sympathy with the intermittent excitation from the retina (Mundy-Castle, 1953; Smythies, 1960, personal comm. from P.E.K. Donaldson; Cragg and Temperly, 1954). The mutually excitatory and inhibitory connections among retinal and/or cortical cells would permit the formation of distinct activity domains and their possible wave-like flow across cortical tissue. The patterns observed would be the result of the reverse mapping, from cortical to retinal space, of the cortical "waves". The hypothesis is attractive in light of recent knowledge of the retino-cortical mapping. We shall return to it in discussing Cowan's (1982) major development of this concept.

[4] The fourth and perhaps most speculative hypothesis is Grey Walter's scanning proposal. Smythies (1960) attempts to test this in two ways. First he investigates the effect of suddenly doubling or halving the flash frequency. Pattern "grain" tended to become, respectively, finer or coarser, consistent with the hypothesis. Second, he used random flicker whose average rate was within the appropriate range. "The patterns appeared to be trying to follow any regularity there was in the random flicker", again consistent with the scanning hypothesis. But Smythies' efforts to obtain more quantitative results by varying the degree of randomness were inconclusive.

Much of the work since Smythies has concentrated on psychophysically measurable aspects of the patterns. Remole (1971) found that the log threshold luminance for first seeing some pattern increased roughly linearly with flicker frequency, but with a wavelength dependence. Again in threshold experiments, Remole (1973) presented evidence that distinctly geometrical patterns originate above the level of binocular interaction, whereas more irregular or diffuse patterns may not. Welpe (1975) found similarly that the checkerboard pattern could only be produced binocularly. Young *et al.* (1975) measured thresholds for the grid and honeycomb patterns, concluding they have different mechanisms and, further, that they do not arise from shadows cast by features of retinal anatomy.

Cowan (1982) gives a mathematical theory of the origin of drug-induced hallucination patterns, and by implication all patterns exhibiting the form constants. Concluding that the form constants are generated in the visual cortex, he shows how the approximate complex logarithmic mapping (Schwartz, 1977) from retina to cortex implies that (1) the cobweb hallucination corresponds to a square lattice parallel to cortical axes, (2) tunnels and funnels correspond to stripe patterns

parallel to the axes, and (3) spirals correspond to stripes not parallel to the axes. Only the patterns of Klüver's type (a), grating, ..., honeycomb, etc., do not have simple cortical correspondents. Thus the geometry of (many of) the form constants arises from their being mappings from cortical to retinal space of even simpler forms cortically.

With several assumptions, Cowan then shows mathematically that if the cortical cell populations are coupled laterally and they are perturbed, states of activation (solutions of the evolution equation) can arise which have the (cortical) pattern of lattices or stripes. Normally, apart from local activity (which Cowan associates with focal attention), the cortex would have a uniform activation state. But hallucinogenic drugs could lessen the ratio of inhibitory to excitatory coupling permitting small perturbations to initiate switches to and between the patterned states.

This idea adds important substance to hypothesis [3], above. However, it is possible that strobe imagery, while sharing the retino-cortical geometry with drug and other hallucinations, differs from them in the nature of its cortical origins. For example, Cowan does not explicitly treat (1) the frequently seen flower or mandala pattern, or (2) imagery that undergoes sustained, rapid, large-scale movement such as rotation or expansion. Perhaps it can be demonstrated that these correspond to more complex cortical states.

3. Toward a New Scanning Model

Development of the present model had two main motivations. First, from the perpective of the retino-cortical mapping, the dynamics of several of the strobe patterns is very suggestive. As noted, a spiral centered at the retinal origin maps into a straight line on the cortex. But a rotating spiral corresponds to moving the line over the cortex in a direction perpendicular to its length. Similarly, an expanding set of circles maps into moving straight lines. For both patterns the cortical correspondent is simple and suggests scanning. (But unlike Walter's "scanning point", the active locus would be a line (or lines), and the scan more like a sweep.)

Second, cortical scanning of the right type could be useful for pattern recognition. The complex log approximation to the retino-cortical mapping has an interesting "size-normalizing" property. If a given retinal image is magnified about the center of vision, the cortical "image" does not basically change in size or shape; instead it translates uniformly along the cortex. This is essentially because under a log transformation, a scale factor M is converted to an additive constant $\log M$, which then functions as the translational offset. Wilson (1983, 1985) pointed out

that the size-normalizing property could be useful for pattern recognition if the translational offset were compensated by some form of scan along that direction.

3.1 Experimental Observations

To gain fresh information in constructing the model, new observations of strobe imagery were made by 23 male and female subjects ranging from 10 to 74 years in age. A GenRad 1539-A strobe was the light source, and subjects observed with closed eyes from a distance of about one inch. In contrast to the procedure of Smythies and others, subjects themselves controlled the flash frequency; the idea was to permit full development of images, and to allow time to examine them in detail. The experimenter controlled intensity, in three steps, always starting at the lowest. Intensities which caused a subject the slightest discomfort were avoided. (Prior to sessions subjects were asked about sensitivity to flashing lights or history of seizures in themselves or their families; all responded negatively.) Starting at 10 hz, subjects were asked to explore gradually the frequency range in both directions and report verbally anything "interesting" as to its "pattern, motion, or color". Subjects could also stop and draw their images.

In very large part, the results confirmed observations of previous workers and so will not be discussed in detail. However, the principal results influencing the construction of the model may be summarized as follows:

> [1] A rather clear separation can be made between "linear" (containing parallel straight or wavy lines) and centrally symmetric imagery. Linear tended to appear at lower intensities, and its motions were translational; centrally symmetric appeared at higher intensities, and its motions were rotational or radial. The two types could be present together, but if so it was as though the linear overlay the other.
>
> [2] Centrally symmetric forms could be divided into "Crosses": (1) crossing vertical and horizontal members (+ sign), (2) crossing diagonals (×), (3) patterns of radial vanes, and (4) a four-fold flower or rosette-like pattern; and "Spirals": (1) single-arm spirals having multiple turns (like a snail's shell), and (2) multi-arm spirals not tightly wrapped (something like a turbine fan). See Figs. 1 and 2.
>
> [3] There was often a mosaic-like ground which at lower intensities tended to be linear (equal sized tiles) and at higher to be centrally symmetric with tiles that seemed larger away from the center. The tiles were usually of many different, constantly changing colors.

Crosses and Spirals appeared to be made of mosaic tiles; that is, they consisted of tiles which were brighter, darker, or colored differently from the others and so stood out. Vivid, varied colors were seen by all but one subject.

[4] Motion types for centrally symmetric imagery included Radial: (1) expansion or contraction of Spiral forms, (2) "flow" of tiles, inward or outward, along Cross arms, (3) expansion from the origin of sets of concentric circles, and (4) radial flow of the entire mosaic; and Rotational: (1) rotation of Spirals and Crosses, and (2) rotation of the entire mosaic, all about the field center. Nine subjects reported seeing these motions in depth, as though in a "tunnel".

[5] Motions were often multiple, as though superposed. For example, while a Cross slowly rotated, some tiles of its arms might appear to be flowing outward. Or some tiles of a mosaic pattern might be converging while others stood still.

[6] There was no clear relationship between flash frequency and the occurrence of patterns or their rates of motion, except that imagery was generally contained in the interval $8 - 20$ hz. Well-organized patterns emerged unpredictably and dissolved or "switched" just as unpredictably—though a person could sometimes recover a pattern by returning to the same frequency later, and people who got patterns easily could hold them and sometimes even change, say, a Spiral's direction of rotation "with their mind".

3.2 The Basic Model **M0**

In arriving at the model we disregarded the linear imagery on the assumption that distinct other processes are responsible. Modeling the centrally symmetric patterns requires a representation of the retino-cortical mapping and we use a slight modification of Wilson's (1983) picture (Fig. 3). This picture is highly schematic but has the advantage that the discreteness of the imagery (the mosaic) is already contained in it. The "retina" of Fig. 3a consists of "data fields" whose size and spacing increase linearly with distance from the center of vision. The "cortex" of Fig. 3b is a matrix of identical "message sending units" (MSUs), each of which receives signals from its own retinal data field, processes the signals, and sends onward a relatively simple output message.

The MSUs are identical with cortical "hypercolumns" (Hubel & Wiesel, 1974) and the data field is identical with the hypercolumn's "aggregate receptive field"

(Hubel & Wiesel, 1979). Wilson's (1983) different terminology is due to his hypothesis (based on characteristics of peripheral vision; see also Frisby (1979) for an apparently similar hypothesis) that the hypercolumn is a strong information-reducer making at any moment a simple output statement drawn from a small set of possible messages. Since the hypercolumn has finite size, this implies that the processing performed by the mapping as a whole is spatially discrete.

The mapping's pattern of connections is as suggested by the letters in Fig. 3. Data fields along a ray from center to periphery map into a row of MSUs, and simultaneously, each ring of data fields maps into a column of MSUs. The leftmost column corresponds to the innermost ring, the 12 o'clock ray maps into the top row, and so forth. The mapping illustrated is complex logarithmic because retinal azimuth angle and the log of radial distance from the center of vision map into cartesian row and column coordinates. There is a singularity at the retinal origin which can be dealt with by beginning the mapping at a finite radius. (According to Schwartz (1983) the complex log approximation is good to within 0.3 deg of the center).

Model **M0** has two main components:

> [1] A retinal array (RA) of data fields as in Fig. 3a, shown again in part in Fig. 4a. From psychophysical data Wilson (1983) estimates the angle between rays of data field centers to be approximately 1/8 rad, or about 50 data fields per circumferential ring. That is roughly within the size range for mosaic tiles suggested by subjects' comments and drawings. We explicitly assume the tiles correspond to data fields.
>
> [2] A pair of fan-like sets of "scanning arms", shown in Fig 4b. The first fan, "L", rotates counterclockwise and its arms curve clockwise outward. The second fan, "D", is the mirror image of L and it rotates clockwise.

The components of the model are "assembled" by placing L and D on top of RA with all three centers coincident (Fig. 4c). In **M0**, there is a strict relationship between the form of L and D and the form of RA. Let $2N$ denote the number of rays of data fields in RA. Then the number of arms in L (and D) is made $N/3$ (a whole number), and they are equally spaced. In addition, each arm is spiroform and falls across the centers of RA data fields such that if an arm crosses the data field at ring i, ray j, the adjacent data fields crossed by that arm have indices $i-1$, $j-1$ and $i+1$, $j+1$ in the case of L, and $i-1$, $j+1$ and $i+1$, $j-1$ for D.

Figure 4c shows the model from the point of view of retinal space. However, the scanning action actually takes place cortically. The corresponding cortical picture

is shown in Fig. 5. The arms of L and D are transformed by the mapping into two sets of diagonal straight lines moving upwards and downwards, respectively, across the MSUs of the cortex. *Whenever an intersection of an L arm and a D arm falls near the center of an MSU, that MSU's message is sampled or "read out" to higher cortical processing levels.* The content of the message depends on the stimulus falling at that moment on the corresponding data field. Thus Fig. 4c also represents the scanning process. As L and D rotate, their intersections move generally outward and can be thought of as sampling the data fields which lie under the intersections. Though the sampling occurs cortically in this model, we shall usually find it convenient to take this retinal point of view. Referring again to Fig. 4c, it will be noted that at any moment, the arms of L (and D) cover only every third spiroform sector of RA. Similarly, the sampling intersections of L and D sample only every third data field.

3.3 Model **M0** *Under Strobe Illumination*

We now place the model in the experimental situation and assume that the retina is uniformly illuminated with a flashing strobe light. Let the flashing rate be F flashes per second and let the rates of rotation of L and D be V_L and V_D spiroform sectors per second (V_L and V_D are not always equal and they may vary). In each flash, the model will only transmit messages from MSUs whose data fields are sampled by L and D intersections ("$L \times D$") at the moment of the flash. The other MSUs will be silent. Thus the instantaneous perception will be of a spaced array of patches of light.

By the time of the next flash, however, $L \times D$ will have moved to new positions on the array, and to a new set of data fields. Thus a different set of patches of light will in general be perceived next. On the following flash, there will be yet another perceived array of patches, and so on. We now make the *hypothesis that the forms and motions reported by observers resulted from perceptual patterns or gestalten arising out of the succession of these instantaneous arrays of patches of light.*

Figure 6 shows $L \times D$ sampling a certain set of data fields on a particular flash. Let us imagine that on the next flash, $L \times D$ has moved in such a way that its intersections again fall precisely on a set of data field centers (integer shift). A moment's reflection will show that the second set will be either (1) the same as the first, or (2) the set formed by shifting the first set exactly one field in one of the directions shown by arrows in Fig. 6.

In case 1, the perception will clearly be of an array that is stationary. In case 2, it will be of motion in the direction of the shift, provided the flash frequency is in

the range where successive presentations can induce a motion gestalt. Furthermore, the motion, if it is perceived, will be unambiguous in direction. The reason is that each intersection shifts (apparently) by a distance which is only one-third, *i.e.*, less than half, the distance to any other intersection. Thus it is perceptually clear which way the sampled fields are "moving".

The arrow directions in Fig. 6 denote three basic modes of array motion: expansion or contraction; rotation clockwise or counter-clockwise; and flow, outwards or inwards, with a spiral curvature like that of the sampling arms. These modes are the same as some types of motion reported by observers.

3.4 A Photo-Mechanical Simulation

It has been assumed that $L \times D$, on each flash, falls precisely on a set of data field centers. What if this is not true? To find out, and to check the previous ideas, a scanning device was built which simulates the model. It consisted of three photographic transparencies in superposition, illuminated by a strobe lamp on one side and viewed from the other side. The transparency adjacent the stobe had a pattern of clear circular spots on a black ground and resembled Fig. 4a (with $N = 36$). The other two transparencies were mounted on clear plastic disks and had spiral arms like those of Fig. 4b, except that the arms had a clear, finite width of approximately one sector with a smoothly changing transparency cross section. In between arms the disk was opaque. Thus, when superposed, the two transparencies yielded clear intersections about the size of the adjacent spots in the first transparency. Seeing a spot through an intersection was taken to be analogous to the sampling of a data field in the model.

The L and D disks could be independently rotated by separate motors. When the speeds V_L and V_D and the flashing rate F were adjusted so that the movements of $L \times D$ met the integer shift condition discussed earlier, it was found that all the predicted motion gestalts occurred. When the integer shift condition was nearly, but not quite, met, the motion was as for the closest integer shift except for an orthogonal drift. For example, with $F = 10$ hz, $V_L = V_D = 10$ sectors/sec, the motion is radial outwards. If V_L is changed to 9 sectors/sec, the radial flow takes on a slight clockwise rotation.

To understand the relationships, combinations of F, V_L, and V_D were tried until a clear pattern emerged. The results are diagrammed in Fig. 7. The axes represent the ratios V_L/F and V_D/F in sectors per flash. The little arrows are located at positions of integer shift and their directions have the same meaning as in Fig. 6. A small circle stands for a stationary pattern. The dashed lines mark loci in which the pattern is without overall motion but, instead of being stationary, it is chaotic.

These loci correspond to an apparent shift by L or D or both of exactly $1\frac{1}{2}$ sectors; when that occurs, the motion direction is ambiguous and a definite gestalt does not form.

Using Fig. 7, we can read off non-integer shift motions as follows. Within any square formed by dashed loci of ambiguity, if you go from an arrow toward the central circle, the motion retains its direction but gets slower. From one arrow to an adjacent one, the motion stays as fast but changes direction as indicated. Across a locus of ambiguity, the motion passes through the chaotic state.

Fig. 7 permits a crude estimate of the cortical scanning rate. Our observers noted that overall patterns of motion came and went with changes in F of 1 hz or less. Since F is of the order of 10 hz, this is a pattern change within a 10% change in F. In Fig. 7, a change in motion pattern requires a unit change on either or both axes. The implication is that V_L and V_D are at least of the order of $10 \times F$, or 100 sectors/sec.

In using the scanning device, we noted an important further gestalt in regions near horizontal arrows. If the device was set up to give pure rotary motion, the actual figures more closely resembled rotating concentric circles separated by spaces than a uniform rotating array. If now any of the three variables was changed slightly, the circles either began expanding outward or contracting inward. But surprisingly, the pattern then looked less like circles than like a single, highly wrapped spiral expanding or collapsing. There was also a feeling of depth, with the center the far point. Thus it may be that the highly wrapped spiral seen by many observers was actually an expanding or contracting set of concentric circles.

Model **M0** has suggested a mechanism for a number of the images seen by our observers: radial and rotary flow; multiple-arm spirals; single, highly wrapped spirals (perhaps); and the intervals of chaotic activity. But **M0** is achromatic whereas the observers reported vivid colors. Furthermore, no understanding is provided of the Cross phenomena. These questions will be addressed in the following two sections.

4. Color (Model M1)

Observers frequently saw vivid colors with a stimulus which is ordinarily regarded as colorless (or bluish-white). Our *basic hypothesis* in trying to understand this fact is to propose that *the scanning process performs a time-dependent trichromatic analysis of the retinal image.* Under ordinary circumstances this analysis is not evident to us, just as trichromaticity itself is not. But, under the conditions of the experiment, the separate color components tend, stroboscopically, to be revealed.

This hypothesis is incorporated into the model by supposing that L and D, rather than each having $N/3$ (achromatic) scanning arms as in **M0**, instead have $N/3$ scanning arms for each of the three trichromatic components, giving N arms in all per scanner. Figure 8 illustrates this for D; the arms of the three chromatic sets are interlaced: R, G, B, R, G, B, etc. When L and D together scan the image, they rotate oppositely just as in **M0**. But now the arms sample in R, G, and B. In detail this means that each data field of RA is cyclically sampled by L as to its R, then G, then B, information; and at the same time is being similarly cyclically sampled by D.

Since the scanning arms are sampling separate chromatic components, the intersections of $L \times D$ can be thought of as sampling pairs of components (where both members of a pair will sometimes be the same, *e.g.*, R and R). Thus $L \times D$ is like a mosaic of colors, though of course it is not itself colored. Rather, the waveband pairs sampled at each intersection change, mosaic-like, from one intersection to the next. At the same time, since L and D rotate, the intersections move with respect to the data fields of RA.

Figure 9 shows part of $L \times D$ for this new model, **M1**. Intersections are labeled as to the color components sampled. The diagram is similar to that of Figure 6 for **M0**. Moreover, the motion gestalten predicted by Figure 9 for the color case are very similar to Fig. 6's predictions for the achromatic case.

Let us imagine, as we did with Fig. 6, that on one flash $L \times D$ superposes exactly on the data fields of RA and on the next flash has moved so as again to superimpose exactly. It is clear that the effective movement of the RR intersections, for instance, will be exactly one field in the direction shown by one of the little arrows in Fig. 9 (unless $L \times D$ duplicates its prior state). The same will be true of the GG and BB intersections. But these are the same kinds of displacements as were discussed in connection with **M0**. Furthermore, since the RR intersections are spaced by three steps (and similarly for GG and BB), these three colors should display the same set of motion gestalten under the same conditions of V_L, V_D, and F.

Interestingly, for the "mixed-color" (*e.g.*, RG) intersections, the situation is different. Fig. 9 shows that for any such intersection, the next equivalent one is within two steps, not three. Motion gestalten under integer shift cannot occur in this case, since it is ambiguous which way the underlying data field has moved. Thus a working device based on **M1** should show motion gestalts for some of the colors (RR, etc.) and ambiguous or merely pulsating behavior in the others. As noted, subjects sometimes reported interwoven combinations of motion types, or mentioned a feeling of overall motion in a field which was otherwise apparently not moving.

To test these ideas, the monochromatic L and D transparencies in the scanning device were replaced with color transparencies. The latter's arms were made cyan, magenta, and yellow ($-$R, $-$G, and $-$B). (If RGB arms are used, a proper simulation of **M1** requires that L and D be superimposed by projection, which is mechanically much more complicated than our basic device, which works "subtractively".) The resulting intersections of $L \times D$ are "colored" with the complements of the colors in Fig. 9. The behavior should similarly reverse, with $-$R$-$R, $-$G$-$G, $-$B$-$B exhibiting the motion gestalts and the others being ambiguous.

When this device was tested, the motion gestalts predicted in Fig. 9 occurred, under exactly the rate conditions given in Fig. 7. It appeared that the movement was attributable to the "negative" colored intersections ($-$R$-$R, etc.), and not to the others. The display would sometimes simultaneously exhibit a static or pulsating aspect which seemed to be due to the remaining intersections. But detailed observation of the "**M1** machine" was harder than for the **M0** machine. Scrutiny of individual colors tended to break up the gestalts, which reappeared when attention became more general.

In summary, Model **M1** seems fairly consistent with subjects reports of multiply-moving patchworks or mosaics of vivid colors. In the next section we extend the model once more to incorporate the Cross group of phenomena.

5. Cross Imagery (Model M2)

The Cross imagery introduces axes of symmetry to the field of view. The simplest Cross has two straight orthogonal members intersecting at the center of vision. Similarly, the simplest flower pattern has four major "petals" separated by right angles. *We can get these symmetries by adding to* **M1** *the possibility of a spatial "beat" or moire between the scanning arms and the retinal array.*

M1 was formed by having $2N$ rays of data fields in RA and, in L and D, $N/3$ (an integer) arms for each of three scanned colors—N arms in all. For example, in the **M1** machine, $N = 36$, with 12 arms of each color in the scanners. A beat can be obtained by changing the rule slightly (giving us Model **M2**). Instead of the same value of N for both RA and $L \times D$, define N_{RA} such that RA has $2N_{RA}$ rays and define N_{LD} such that L and D each have $N_{LD}/3$ arms in each color; but now let N_{RA} and N_{LD} differ by four. For example, we can keep $N_{LD} = 36$, but make $N_{RA} = 32$. $L \times D$ will then have 72 rays of intersections as before, but RA will have only 64 rays of data fields. Model **M2** thus permits the "wavelength" of the traveling scanning pattern, and that of the sampled array, to differ slightly.

Figure 10 shows the resulting spatial beat. $L \times D$ (in black and white) was superimposed on RA and the combination photographed. A "flower" pattern with

fourfold symmetry is apparent. Note that at any constant distance from the center, $L \times D$ and RA are in phase at four equally spaced places. Note also that along any radius, the two components also go in and out of phase, so that the beat effect holds both radially and in azimuth.

The **M1** scanning machine was modified for model **M2** by changing to an RA with $N_{RA} = 32$. It was immediately apparent that besides the motion gestalts for individual intersections of $L \times D$, there were now separate motion gestalts possible for the "petals" of the flower pattern. That is, groups of intersections forming a petal would appear to move as a unit. As with **M0**, the quantities V_L, V_D, and F were varied until the underlying pattern presented in Fig. 11 was found (the pattern can be explained in detail analogously to Fig. 7).

Arrows and small circles in Fig. 11 have the same significance as in Fig. 7. Interestingly, the stationary points of the beat pattern occur for every integer pair of V_L/F and V_D/F, instead of at integer values divisible by three. Both charts apply, however, so it is quite possible to have an operating point (say, $V_L/F = 1$, $V_D/F = 2$) showing, for example, rotation of the intersections but no movement of the flower pattern. The arrows in Fig. 11 are drawn quite close to the stationary points. It was found that small movement away from the latter would throw the flower pattern into strong radial or rotational movement. Again, this could be at variance with perceived intersection flow as given by Fig. 7. All these effects correlate well with our subjects' reports, which included expanding, converging, and rotating motions of the Cross images, together with "flow" within the Cross arms.

There was a surprise in working with the **M2** machine represented by the small letters "p" at half-integer values of V_L/F and V_D/F. The p stands for "pinwheel" in the fireworks sense, and that describes the effect. Figure 12 shows a diagram: there are four comet-like curving arms; at a point slightly away from the points p, the figure slowly rotates while "light" appears to flow out the arms. Our subjects made some reports of multi-arm, or fan-like, spiral figures. Earlier we associated these with states of **M0** represented by diagonal arrows in Fig. 7, that is, gestalts of flow along scanner arms. This explanation may be incomplete, however, because the fan-figures predicted by Fig. 7 are not easily made to appear rotating, while many of the reports mentioned slow rotation. Thus the pinwheels of **M2**, which do readily rotate, may be more properly associated with what some subjects saw. Perhaps these are the "Catherine wheels" (fireworks pinwheels) seen by Walter's subjects.

6. Discussion

The models give an account of much of the centrally symmetric imagery, but not all. Two figures incompletely explained are:

> [1] The tightly wrapped spiral. As noted, sometimes this may have been concentric circles in radial motion. But the drawings suggest a true spiral was often clearly seen. The right- or left-handed sense of these spirals is a kind of asymmetry which apparently cannot be obtained from the models as they stand, but could be obtained by making the pitch of L's arms different from D's.
>
> [2] Examples of the Cross class which are not flower-like. Again, pitch changes would give the straight-arm Crosses; here, the pitches of both L and D should be equal and greater (straighter arms). Both this change and that of [1] amount cortically to changing the angle, and equally the direction of motion, of the scan lines.

An important question not addressed by the scanning model is why strobe patterns tend best to be seen in spatially uniform light. A strobe-lit ordinary room tends not to show the imagery. Conceivably, the perception of objectively existing forms in the field of view easily dominates perceptions arising from the scanning mechanics *per se*. For example, stationary features of the room would conflict with imagery movement gestalts; scanning effects may only be perceivable in the absence of such conflicts. Observations of intermittent stimuli related in form to Fig. 3a could be relevant to this speculation.

It should be pointed out that while the models employ "scanners", L and D actually have no phase. That is, as they sample the MSU outputs, there is no distinguishable mark that cycles repetitively across the cortex, or from the center of vision to the periphery. Rather, L and D are a convenient way of describing a certain spatio-temporal sampling pattern that is locally scan-like, but has no beginning or end (*i.e.*, phase) with respect to the striate cortex as a whole.

We could obtain a "phased" system, at least in principle, by giving L and D definable orientations. The simplest way is to choose an arm of each and label it, say, the "zero arm". The two zero arms will have an intersection which we can label, say, "x". If L and D counterrotate at equal speeds, x will move from center to periphery along some radius. To select another radius we could briefly let L go a little faster then return its speed to that of D. In this way a "scan" of well-defined phase and azimuth would be set up. Such a scan, if it exists, could assist the retino-cortical mapping's size-normalizing property noted earlier. Walter apparently had in mind a "phased" scan but this additional assumption has not been necessary in our proposed explanation of the imagery. (In fact, the present model is perhaps

more appropriately termed a "sampling", rather than "scanning", model; but use of the latter term greatly simplified the model's exposition.)

The present, "unphased" model would predict that if the strobe light stimulated just one set of color receptors, then only that color should be seen in centrally symmetric imagery, and the patterns should have voids corresponding to MSUs being sampled for the other wavelengths. In effect the patterns should be like those of the achromatic model **M0**, except they would be monochromatic. Smythies (1959b) used ordinary photographic filters in his color tests and it is not clear whether the results were monochromatic or not. Brown and Gebhard (1948) state that certain color patterns were the same with and without filters, but their experiments were monocular, raising questions about the contribution of the dark eye. In a preliminary experiment with one subject who in white light easily sees many colors, and using special sharp cutoff bandpass filters centered on the photopigment peaks we obtained results supportive of the model's prediction.

A "phased" model would predict that the time of perception of events in the periphery would depend on the phase of the scan. Our model as it stands would not predict such a dependence on time; this is consistent with the little evidence available (*e.g.*, Walsh, 1952, MacKay, 1953; see also Harter, 1967). Given the potential relevance to pattern recognition, however, the question should be further tested. Walter believed that scanning might be based on the alpha rhythm. Varela *et al.* (1981) found that perception of a two-LED apparent motion stimulus correlated markedly with alpha rhythm phase, one of the first cases in which the latter has been positively tied to an example of "perceptual framing". Perhaps a modification of their experiment, with the LEDs in the periphery, would show the dependence on eccentricity that "phased" scanning predicts.

7. Conclusion

This paper has investigated the striking and incompletely explained phenomenon of stroboscopic imagery, a phenomenon which may offer important clues to visual function. A theoretical model has been presented based upon a postulated trichromatic cortical sampling process, and it has been shown that much of the imagery can be accounted for by the model. Potentially, the sampling process provides a basis for time-dependent phenomena such as perceptual framing and flicker fusion effects, and an example of a bridge between vision and brain rhythms.

REFERENCES

Brown, C. R. & Gebhard, J. W. (1948). Visual field articulation in the absence of spatial stimulus gradients. *J. Exp. Psychol.*, **38**, 188-200.

Cowan, J. D. (1982). Spontaneous symmetry breaking in large scale nervous activity. *Int. J. Quant. Chem.*, **22**, 1059-1082.

Cragg, B. G. & Temperley, H. N. V. (1954). The organization of neurones: a cooperative analogy. *Electroenceph. Clin. Neurophysiol.*, **6**, 85-92.

Edridge-Green, F. W. (1920). *The Physiology of Vision.* London: Bell.

Frisby, J. P. (1979). *Seeing.* Oxford University Press.

Harter, M. R. (1968). Excitability cycles and cortical scanning: a review of two hypotheses of central intermittency in perception. *Psychol. Bull.*, **68**, 47-58.

Helmholtz, H. V. (1962). *Treatise on Physiological Optics, Part II*, p. 256. New York: Dover Publications.

Hubel, D. H. & Wiesel, T. N. (1974). Uniformity of monkey striate cortex: a parallel relationship between field size, scatter, and magnification factor. *J. Comp. Neurol.*, **158**(3), 295-305.

— (1979). Brain mechanisms in vision. *Scientific American*, **241**(3), 150-162.

Klüver, H. (1942). Mechanisms of hallucinations. *In Studies in Personality.* New York: McGraw-Hill.

Mackay, D. M. (1953). Some experiments on the perception of patterns modulated at the alpha frequency. *Electroenceph. Clin. Neurophysiol.*, **5**, 559-62.

Mundy-Castle, A. C. (1953). Electrical responses of the brain in relation to behavior. *Brit. J. Psychol.*, **44**, 318-329.

Purkinje, J. E. (1823). *Beobachtungen u. Versuche zur Physiologie der Sinne. Beitraege zur Kenntnis des Sehens in subjectiver Hinsicht.* Bd. I, Prag.

Remole, A. (1971). Luminance thresholds for subjective patterns in a flickering field: effect of wavelength. *J. Opt. Soc. Amer.*, **61**, 1164-1168.

— (1973). Subjective patterns in a flickering field: binocular and monocular observations. *J. Opt. Soc. Amer.*, **63**, 745-748.

Schwartz, E. L. (1977). Spatial mapping in the primate sensory projection: analytic structure and relevance to perception. *Biological Cybernetics*, **25**, 181-194.

— (1983). Cortical mapping and perceptual invariance: a reply to Cavanagh. *Vis. Res.*, **23**, 831-835.

Siegel, R. K. (1977). Hallucinations. *Scientific American*, **237**(4), 132-140.

Smythies, J. R. (1957). A preliminary analysis of the stroboscopic patterns. *Nature*, **4558**, 523-524.

— (1959a). The stroboscopic patterns. I. The dark phase. *Brit. J. Psychol.*, **50**, 106-16.

— (1959b). The stroboscopic patterns. II. The phenomenology of the bright phase and after images. *Brit. J. Psychol.*, **50**, 305-24.

— (1960). The stroboscopic patterns. III. Further experiments and discussion. *Brit. J. Psychol.*, **51**, 247-255.

Varela, F. J., Toro, A., John, E. R., Schwartz, E. L. (1981). Perceptual framing and cortical alpha rhythm. *Neuropsychologia*, **19**, 5, 675-686.

Walsh, E. G. (1952). Visual reaction time and the alpha-rhythm: an investigation of a scanning hypothesis. *J. Physiol.*, **118**, 500-8.

Walter, W. G. (1950). Features in the electro-physiology of mental mechanisms. In *Perspectives in Neuro-Psychiatry*, edited by D. Richter. London: Blackwell Scientific Publications.

— (1953). *The Living Brain.* New York: W. W. Norton.

Welpe, E. (1975). Das Schachbrettmuster, ein nur binokular anregbares Flimmermuster. *Vis. Res.*, **15**, 1283-1287.

Wilson, S. W. (1983). On the retino-cortical mapping. *Int. J. Man-Machine Studies*, **18**, 361-369.

— (1985). Adaptive "cortical" pattern recognition. *Proceedings of an International Conference on Genetic Algorithms and Their Applications.* Grefenstette, J.J., ed., Pittsburgh: Carnegie-Mellon University.

Young, R. S. L., Cole, R. E., Gamble, M., & Rayner, M. D. (1975). Subjective patterns elicited by light flicker. *Vis. Res.*, **15**, 1291-1293.

FIGURE CAPTIONS

Fig. 1 Examples of cross-like patterns re-drawn by the author from subjects' drawings. (Actual sizes in this and following figure typically 5-10 cm in diameter.)

Fig. 2 Examples of spiroform patterns from subjects' drawings.

Fig. 3(a) Schematic retina showing "data fields", each of which sends signals to its corresponding "message sending unit" (MSU) in the schematic cortex of (b). The MSU labeled F, for example, receives information about the stimulus falling on data field F, processes the information and generates a simple output message summarizing the overall form of that stimulus. (Data fields would overlap at least enough for complete coverage; for clarity they are shown non-overlapping.)

Fig. 4 Components of basic scanning model **M0**. (a) Data fields of a fragment of the retinal array RA. (b) The scanners L and D. (c) Arms from L and D shown in relation to the RA fragment of (a) at some instant.

Fig. 5 Cortical correspondent of Fig. 4. Solid scan lines correspond to D; dashed lines to L. Circles indicate MSUs connected to the data fields of RA. Scanning actually occurs cortically, on the outputs of the MSUs, but retinal viewpoint (Fig. 4) is usually taken in text.

Fig. 6 $L \times D$ sampling a certain set of data fields (dots indicate data field centers). Arrows: possible perceived directions of array movement in case $L \times D$ again falls on data field centers at next flash.

Fig. 7 Perceived array motion for Model **M0** as a function of V_L/F and V_D/F in sectors per flash. Up vertical arrow stands for expanding radial flow; down for contracting. Left-pointing horizontal arrow stands for counterclockwise rotary flow; right-pointing for clockwise. Diagonal arrows indicate flow along spiral arms. See text for further explanation.

Fig. 8 Some scanning arms of D according to Model **M1**, with each arm sampling either R or G or B (red or green or blue chromatic components).

Fig. 9 $L \times D$ for Model **M1** with intersections labeled as to pairs of chromatic components sampled.

Fig. 10 A spatial beat pattern obtained by superposing $L \times D$ with $N_{LD} = 36$ upon RA with $N_{RA} = 32$, in accordance with Model **M2**.

Fig. 11 Perceived motion of beat pattern in Model **M2** as a function of V_L/F and V_D/F in sectors per flash. Arrows have same directional significance as in Fig. 7, but here refer to motions of beat pattern. See text for further explanation.

Fig. 12 Drawing of "pinwheel" pattern seen in the **M2** machine at points p in Fig. 11 for which V_L/F takes half-integer values.

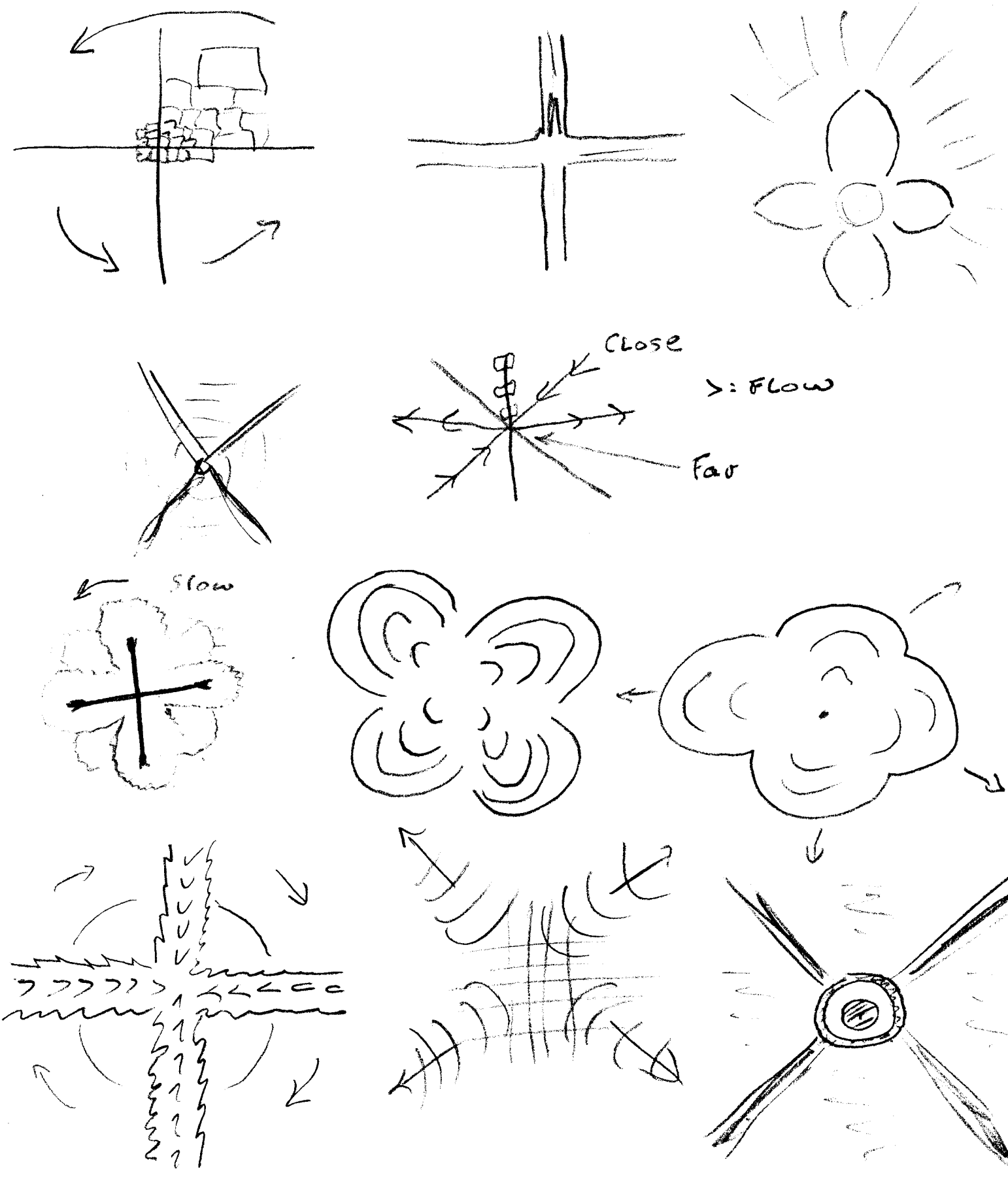

Fig. 1

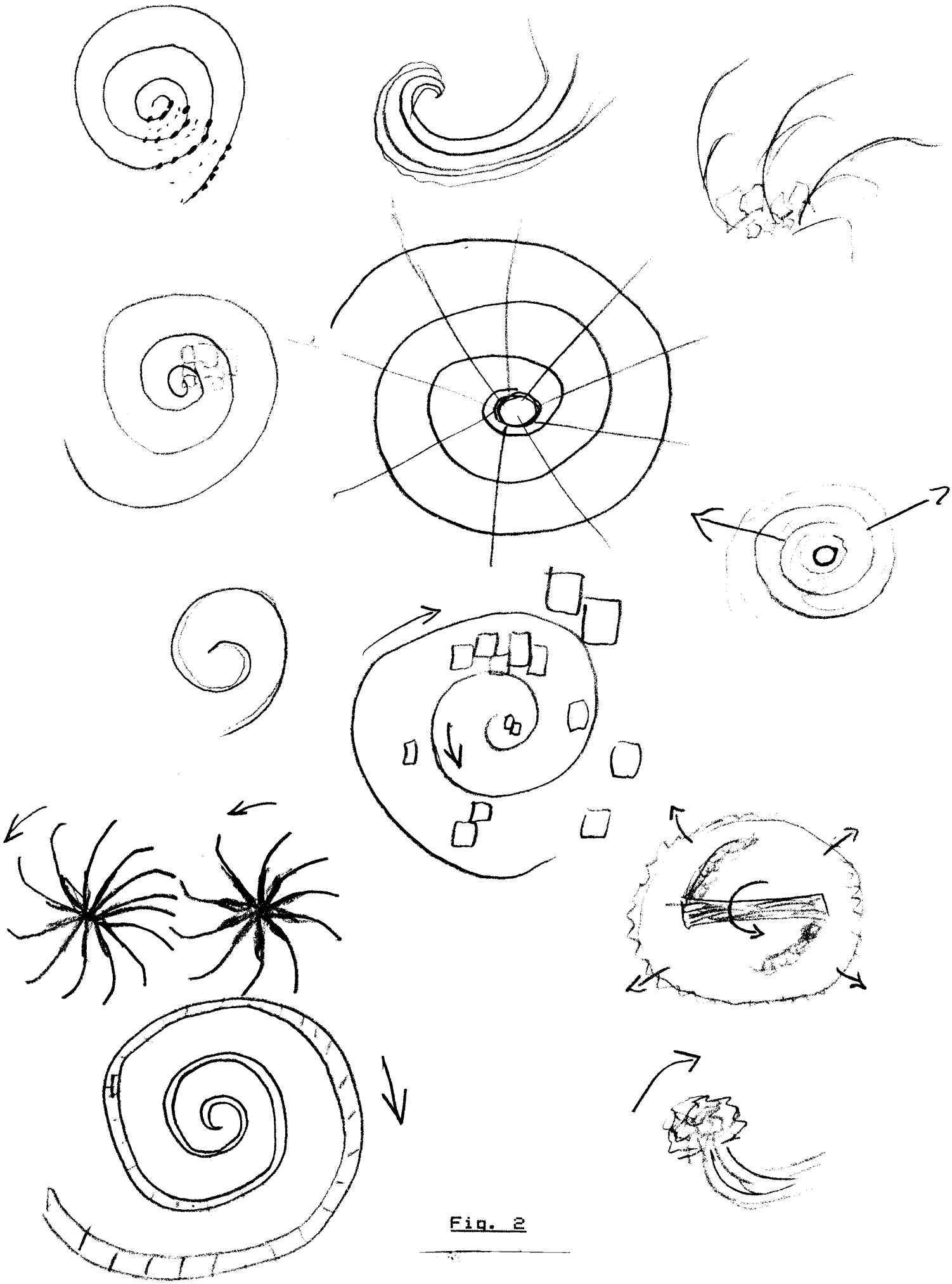

Fig. 2

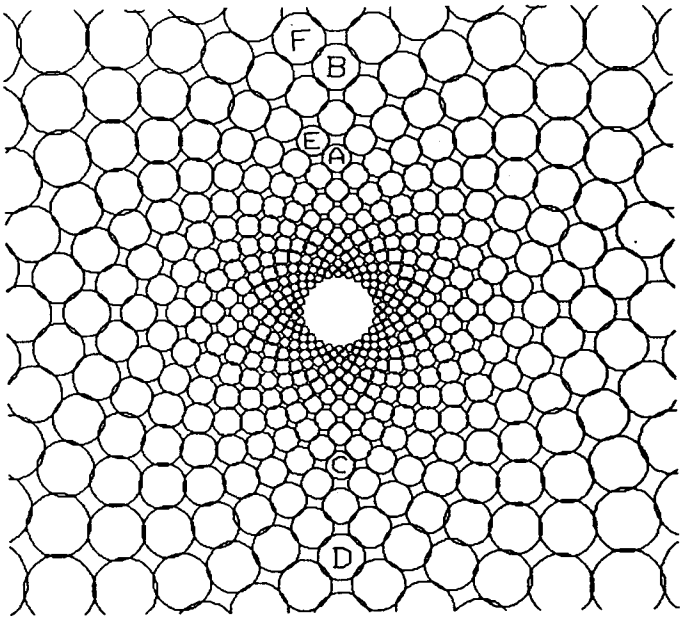

(a)

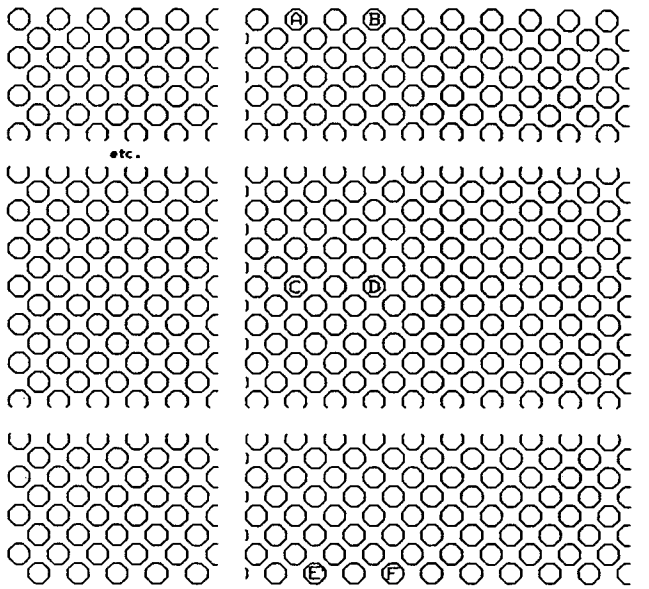

(b)

Fig. 3

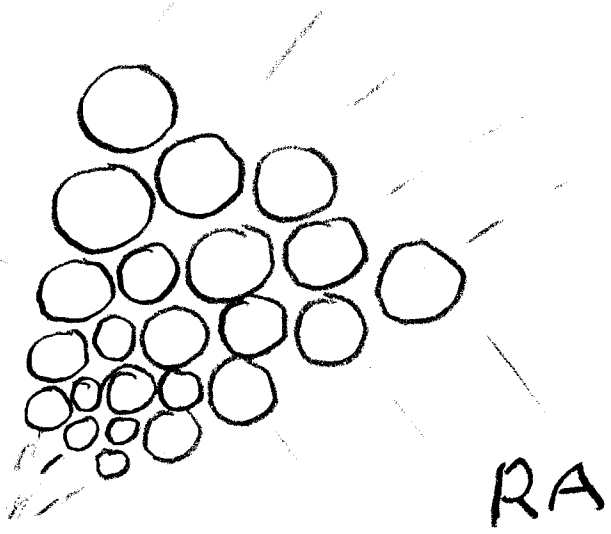

a

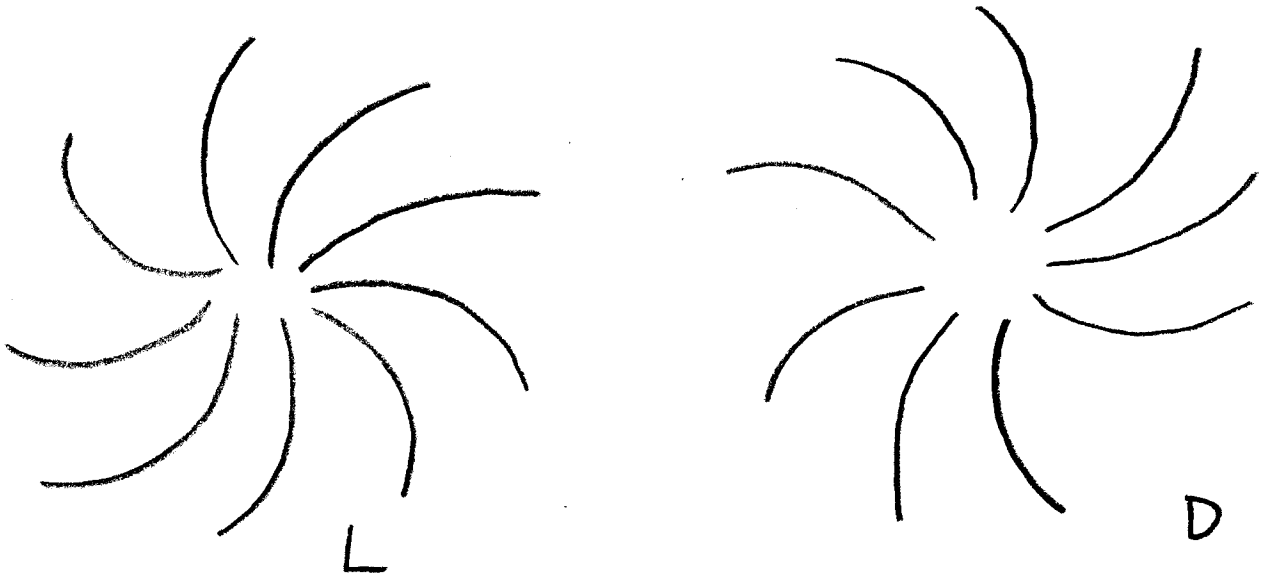

b

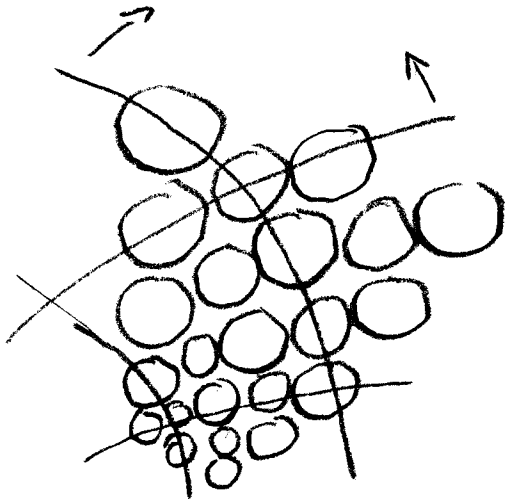

c

Fig. 4

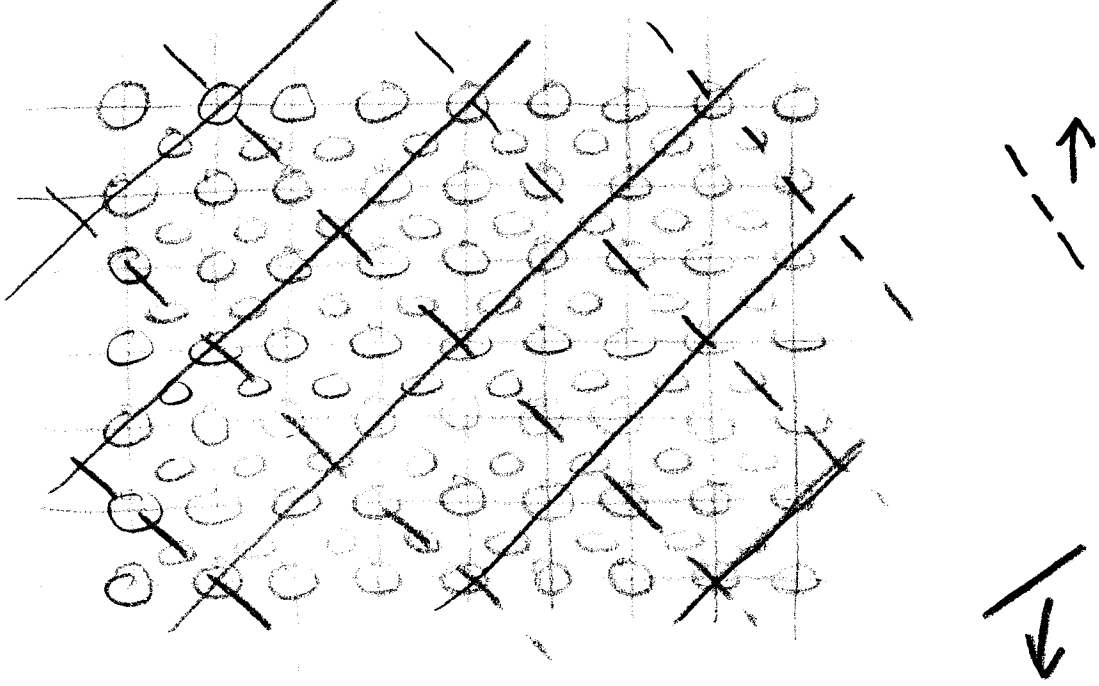

Fig. 5

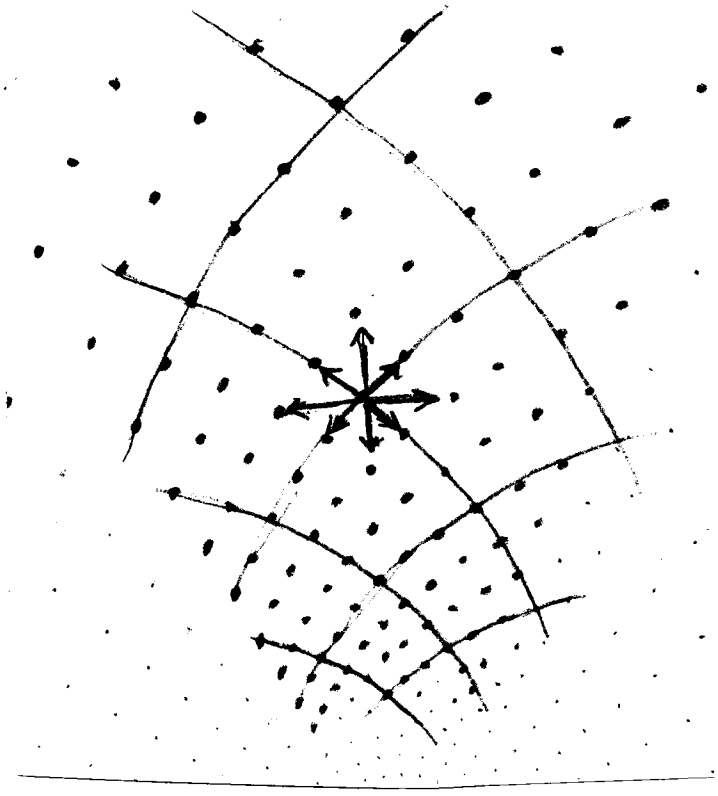

Fig. 6

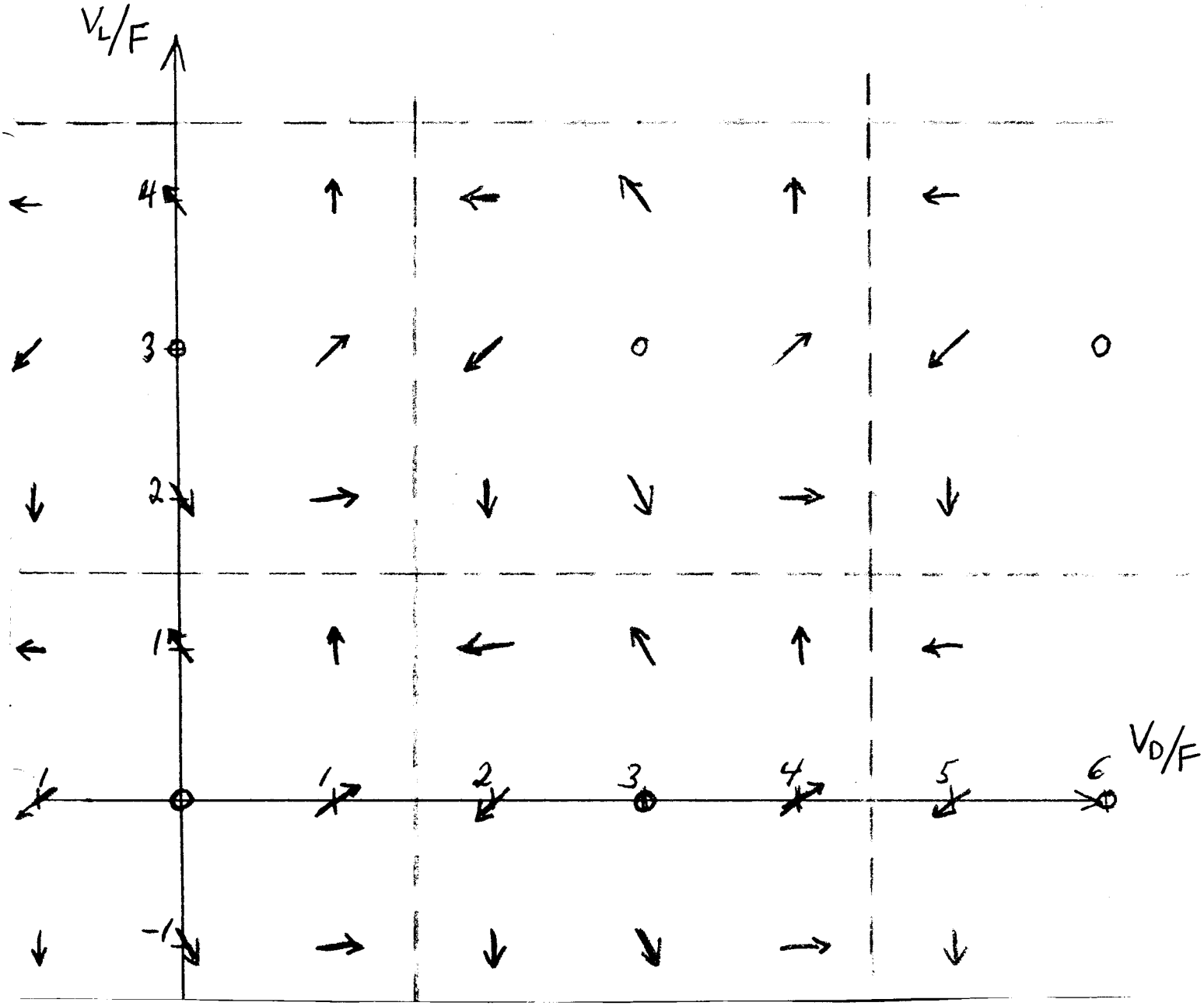

Fig. 7

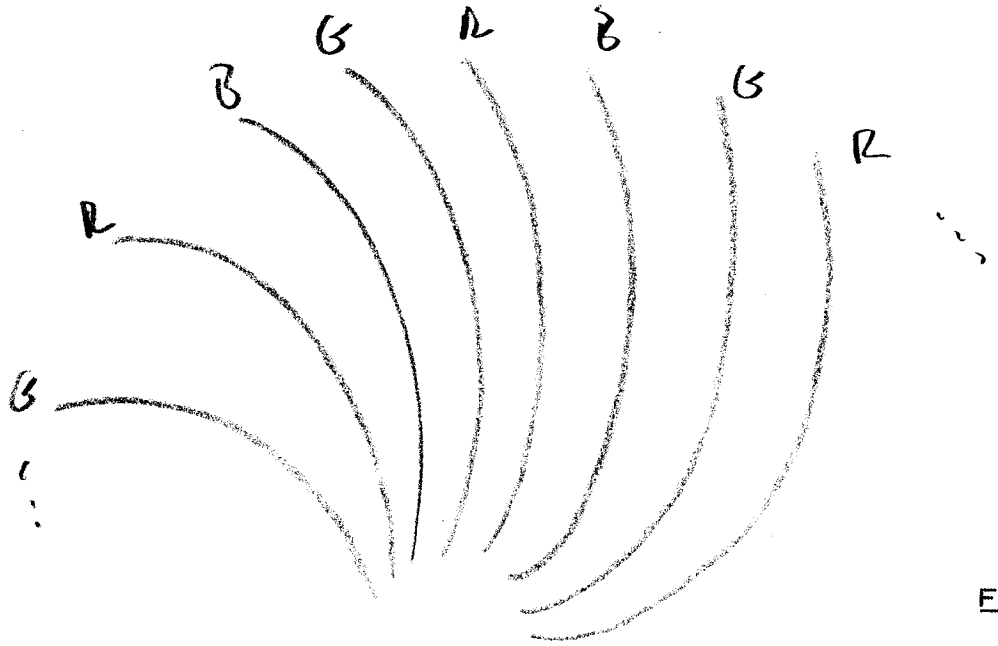
G
R
B
G
B
R
G

Fig. 8

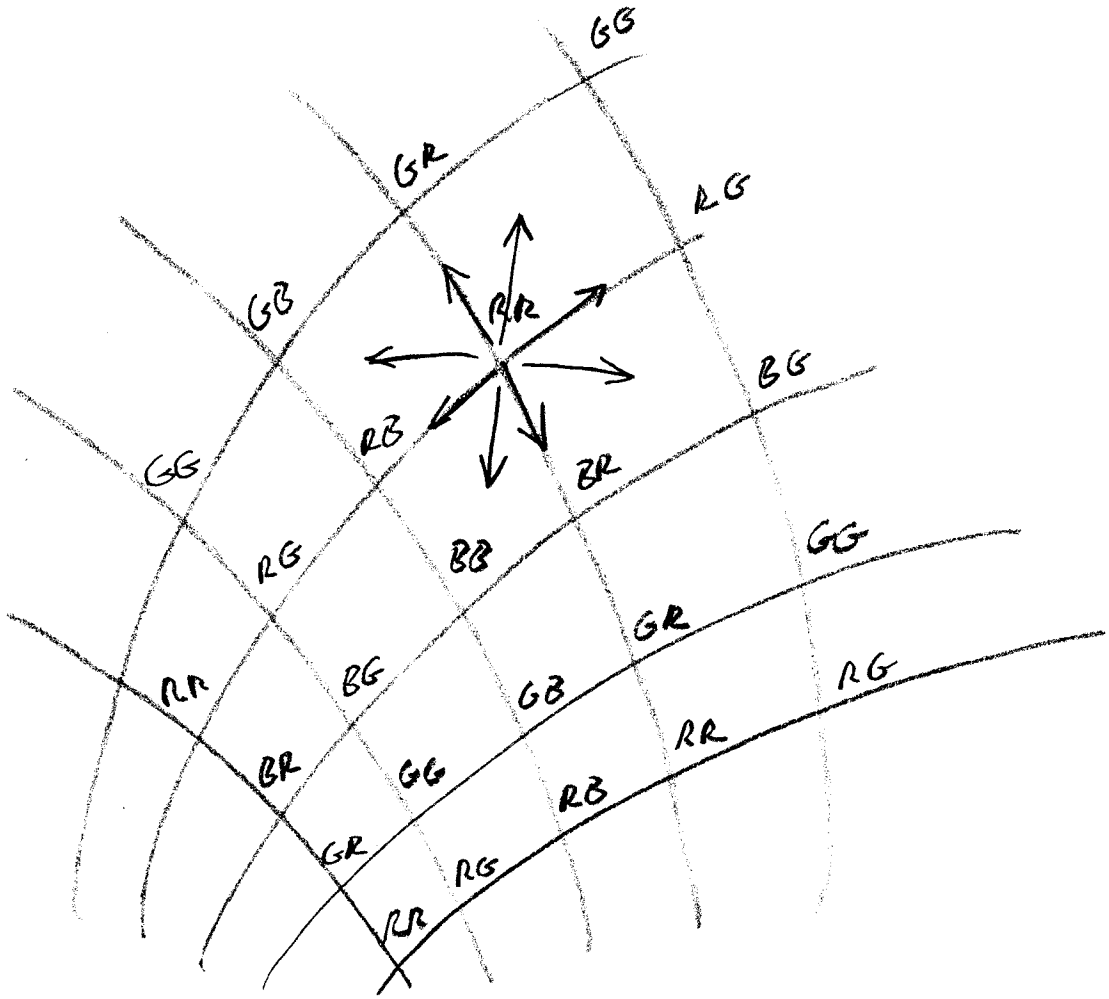
GG
GR
RG
GB
RR
BG
RB
BR
GG
RG
BB
GG
GR
RR
BG
GB
RG
BR
GG
RR
RB
GR
RG
RR

Fig. 9

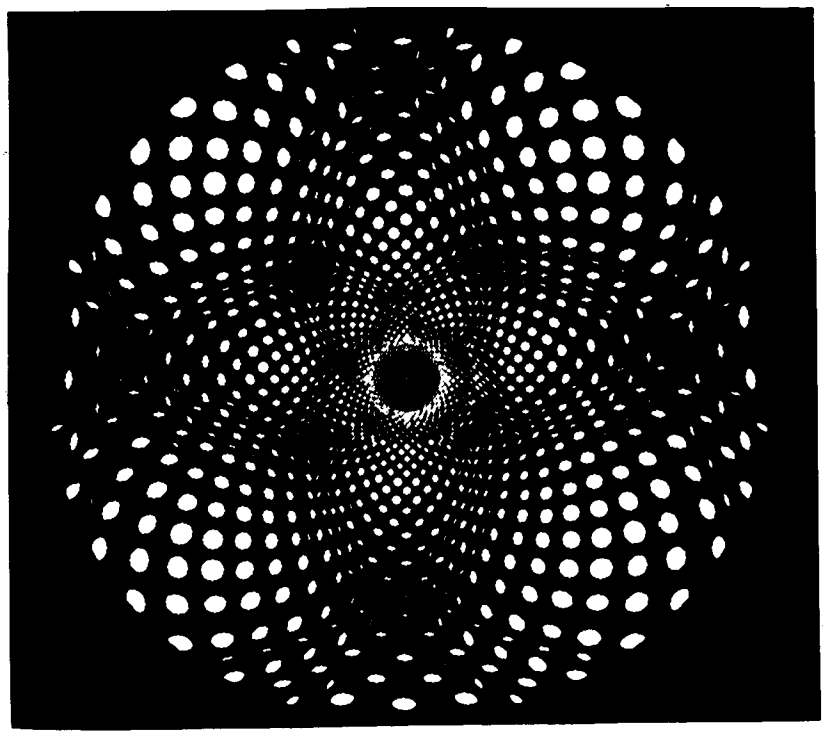

Fig. 10

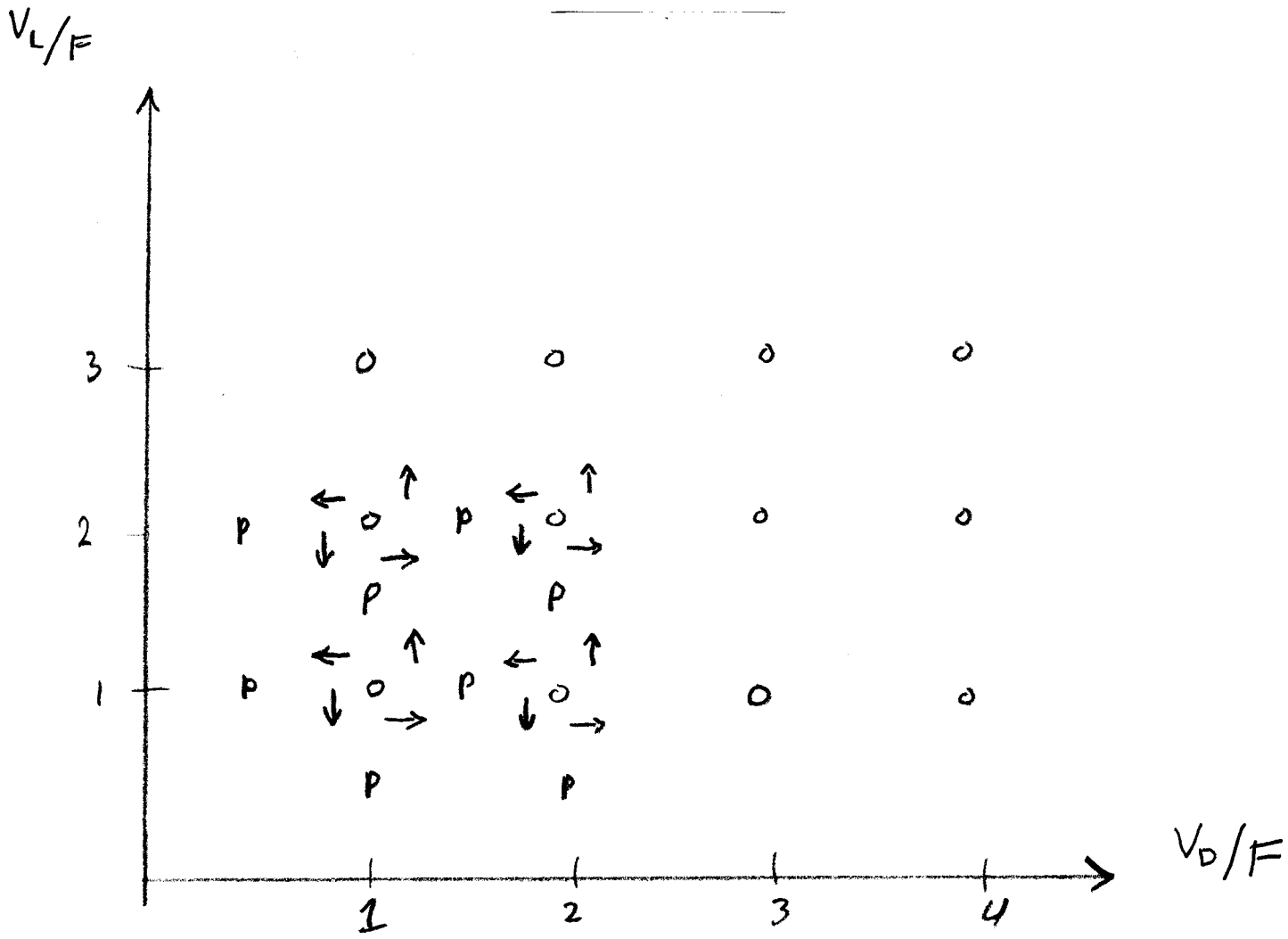

Fig. 11

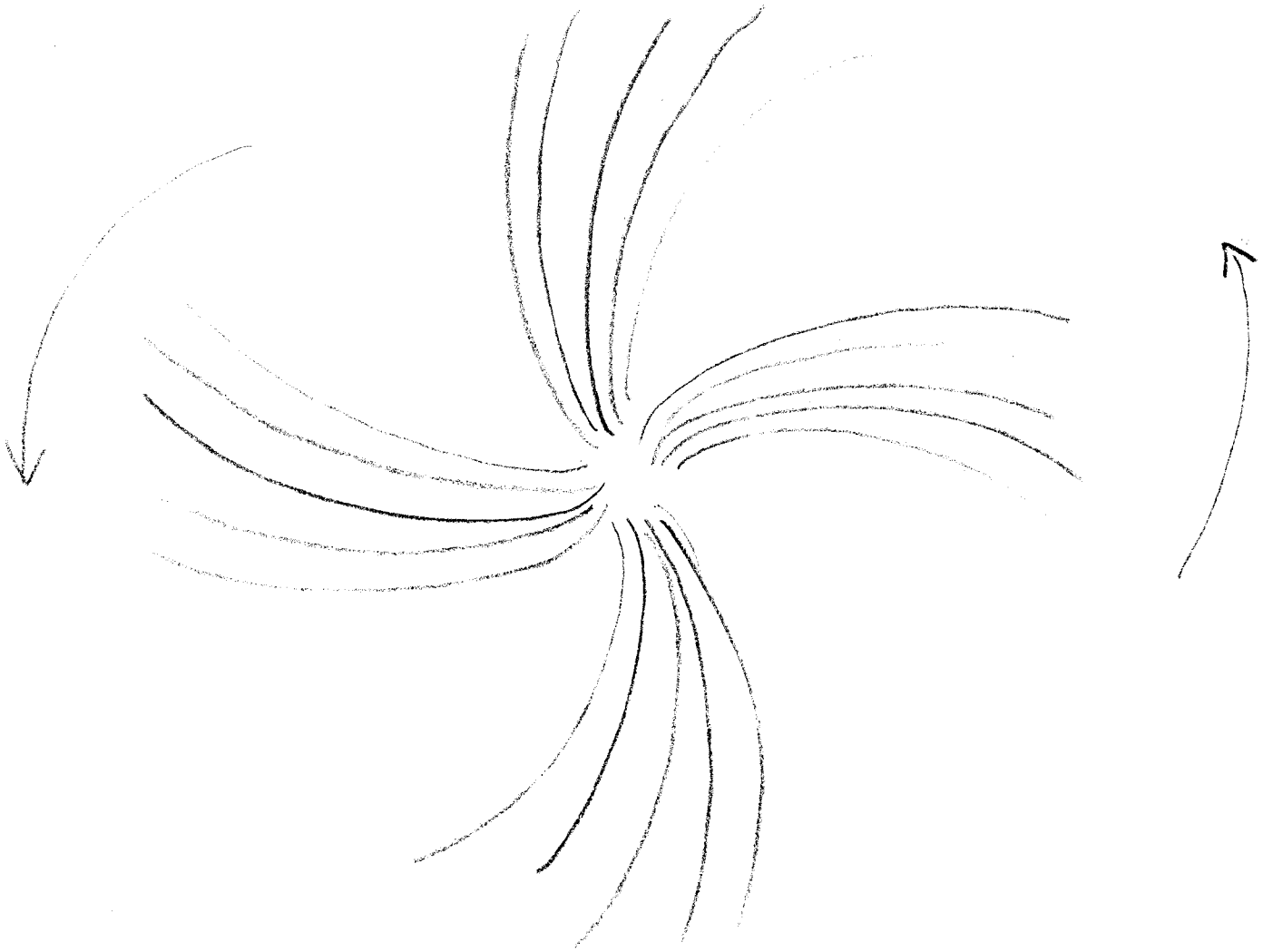

Fig. 12